THE JOURNAL OF BIOLOGICAL CHEMISTRY
Vol. 276, No. 46, Issue of November 16, pp. 43145–43151, 2001

Printed in U.S.A.

Design and Characterization of a Highly Selective Peptide Inhibitor of the Small Conductance Calcium-activated K^+ Channel, SkCa2*

Received for publication, July 24, 2001, and in revised form, August 29, 2001
Published, JBC Papers in Press, August 29, 2001, DOI 10.1074/jbc.M106981200

Vikram G. Shakkottai‡§¶, Imed Regaya§‖, Heike Wulff‡, Ziad Fajloun‖, Hiroaki Tomita‡, Mohamed Fathallah‖, Michael D. Cahalan‡, J. Jay Gargus‡, Jean-Marc Sabatier‖, and K. George Chandy‡**

*From the ‡Department of Physiology and Biophysics, University of California, Irvine, California 92697, ‖CNRS Unité Mixte de Recherche 6560, Faculté de Médecine Nord 13014, Marseille, France, and **CIC 9502, Assistance Publique des Hôpitaux de Marseille-INSERM, Hôpital Sainte Marguerite, Marseille 13009, France*

Apamin-sensitive small conductance calcium-activated potassium channels (SKCa1–3) mediate the slow afterhyperpolarization in neurons, but the molecular identity of the channel has not been defined because of the lack of specific inhibitors. Here we describe the structure-based design of a selective inhibitor of SKCa2. Leiurotoxin I (Lei) and PO5, peptide toxins that share the R*X*CQ motif, potently blocked human SKCa2 and SKCa3 but not SKCa1, whereas maurotoxin, Pi1, Tsκ, and PO1 were ineffective. Lei blocked these channels more potently than PO5 because of the presence of Ala[1], Phe[2], and Met[7]. By replacing Met[7] in the R*X*CQ motif of Lei with the shorter, unnatural, positively charged diaminobutanoic acid (Dab), we generated Lei-Dab[7], a selective SKCa2 inhibitor (K_d = 3.8 nM) that interacts with residues in the external vestibule of the channel. SKCa3 was rendered sensitive to Lei-Dab[7] by replacing His[521] with the corresponding SKCa2 residue (Asn[367]). Intracerebroventricular injection of Lei-Dab[7] into mice resulted in no gross central nervous system toxicity at concentrations that specifically blocked SKCa2 homotetramers. Lei-Dab[7] will be a useful tool to investigate the functional role of SKCa2 in mammalian tissues.

Ca^{2+}-activated K^+ (K_{Ca})[1] channels modulate cytosolic Ca^{2+} concentrations in excitable and non-excitable tissues by regulating the membrane potential. Based on their unitary conductance, K_{Ca} channels are classified as BK_{Ca}, IK_{Ca}, and SK_{Ca} (1). Opening in response to an increase in cytosolic $[Ca^{2+}]_i$ in the 200–500 nM range (2), SK_{Ca} channels modulate the firing pattern of neurons by generating slow membrane after hyperpolarizations (3–5). In the liver, they are believed to play a role in metabolic stress responses (6), and in human Jurkat T cells, they promote calcium entry in response to a mitogenic stimulus (7). SK_{Ca} channels have also been implicated in fasciculations in denervated skeletal muscle (8) and in myotonic dystrophy (9). SK_{Ca} channels, products of three phylogenetically related genes *SKCa1–3*, are found in a variety of tissues including the nervous system (10), liver (11), skeletal and smooth muscle (8, 12), adrenal medulla (13), and lymphoid tissues (14, 15). In the brain (16), the precise functional role of each channel in specific neuronal pathways has been difficult to elucidate because of the absence of selective blockers. The identity of the specific SK_{Ca} channel(s) responsible for apamin-induced destruction of cerebellar Purkinje neurons (17) and altered seizure threshold (18, 19) and for apamin and Lei neurotoxicity (20) is also unclear. The development of inhibitors that target each of these channels selectively would facilitate studies to determine their specific roles in mammalian tissues.

The SKCa2 channel is expressed in the brain (10, 16), retina (21), liver (22), melanocytes (expressed sequence tag AA418096), fetal heart (expressed sequence tag AA418000), and human Jurkat T cell line (7, 22, 23). Precise determination of function has only been possible in Jurkat T lymphocytes in which this channel plays a role in calcium signaling (7, 14, 24). The existing blockers of SKCa2 channels are not adequately specific to distinguish this channel from other SK_{Ca} subtypes. Apamin, a peptide from bee venom, exhibits only 10-fold selectivity for human SKCa2 over human SKCa1 or SKCa3 (3, 22, 25, 26), while the bisquinolinium cyclophane UCL-1684 blocks SKCa2 and SKCa1 with roughly equivalent potency (25) although it shows some selectivity over SKCa3 (7). The peptide toxin Lei (also known as scyllatoxin) from the scorpion *Leiurus quinquestriatus hebraeus,* currently the most specific inhibitor of SKCa2, exhibits ~200-fold selectivity for human SKCa2 (15) over SKCa1 (25), although its affinity for SKCa3 had not been determined.

This study describes the guided design and electrophysiological characterization of a novel Lei analog that selectively blocks SKCa2 homotetramers with low nanomolar affinity. Our strategy to design a specific inhibitor of the SKCa2 channel exploited an approach used previously to develop selective blockers of Kv1.3 and IKCa1 channels (27, 28). In this approach, a potent yet non-selective inhibitor of the target channel is the starting template. Specificity for the desired channel is engineered into the peptide on the basis of experimentally determined differences in its interaction with the target channel and other channels. Using Lei and a closely related peptide PO5 as templates, and by comparing the potencies of the native and mutant toxins for SKCa1, SKCa2, and SKCa3, we delineated the channel-binding surfaces of these toxins. Lei-Dab[7] was

* This study was supported by Grant MH59222 from the National Institutes of Health (to K. G. C.), by an American Heart Association Fellowship (to H. W.), and by CNRS and Cellpep S.A. (Paris, France) funds. The costs of publication of this article were defrayed in part by the payment of page charges. This article must therefore be hereby marked "*advertisement*" in accordance with 18 U.S.C. Section 1734 solely to indicate this fact.

§ These two authors contributed equally to this work and should be considered co-first authors.

¶ To whom correspondence should be addressed: Rm. 291, Joan Irvine Smith Hall, Medical School, University of California, Irvine, CA 92697. Tel.: 949-824-2133; Fax: 949-824-3143; E-mail: vshakkot@uci.edu.

[1] The abbreviations used are: K_{Ca}, calcium-activated K^+ channel; SK_{Ca}, small conductance K_{Ca}; BK_{Ca}, large conductance K_{Ca}; IK_{Ca}, intermediate conductance K_{Ca}; Lei, leiurotoxin I; Dab, diaminobutanoic acid; Dapa, diaminopropionic acid; GFP, green fluorescent protein; Fmoc, *N*-(9-fluorenyl)methoxycarbonyl; HPLC, high-pressure liquid chromatography.

designed to target a structural feature unique to the Lei-SKCa2 interaction surface.

EXPERIMENTAL PROCEDURES

Peptide Synthesis—*N*-α-Fmoc-L-amino acid derivatives, Fmoc-amide resin, and chemical reagents used for peptide synthesis were purchased from PerkinElmer Life Sciences (Shelton, CO), Novabiochem (Laufelfingen, Switzerland), and Neosystem Laboratoire (Strasbourg, France). Solvents were analytical grade products from SDS (Peypin, France). The various peptides were synthesized by the stepwise solid-phase method (29) using a peptide synthesizer (Model 433A, Applied Biosystems Inc., Foster City, CA). The side-chain protecting groups used for trifunctional residues were: 2,2,5,7,8-pentamethylchromane-6-sulfonyl for Arg and homoarginine; *tert*-butyloxycarbonyl for Orn, Lys, and homolysine, and 1-(4,4-dimethyl-2,6-dioxocyclohex-1-yliden)-3-methylbutyl for Dab and diaminopropionic acid (Dapa). The reduced peptides were dissolved at 1 mM in 0.2 M Tris-HCl buffer, pH 8.3, and stirred under air to allow folding/oxidation (48 h, 25 °C). The folded/oxidized toxins and their structural analogs were purified to homogeneity by reversed-phase high-pressure liquid chromatography (HPLC) (PerkinElmer Life Sciences), C_{18} Aquapore ODS 20 μm, 250 × 10 mm). The homogeneity (>99%) and identity of the peptides were verified by: (i) analytical C_{18} reversed-phase HPLC, (ii) amino acid content determination after acidolysis, and (iii) mass analysis by matrix-assisted laser desorption ionization-time of flight mass spectrometry.

Cell Culture—Jurkat E6–1, COS-7, and PC12 cells were obtained from ATCC (Manassas, VA). Jurkat E6–1 cells were grown in RPMI medium supplemented with 10% fetal bovine serum, 2 mM glutamine, and 10 mM HEPES at densities of 1–9 × 10^5 in a 37 °C humidified incubator with 5% CO_2. COS-7 and PC12 cells were cultured in Dulbecco's modified Eagle's medium containing 10% fetal calf serum and 2 mM glutamine and split twice weekly. Unless otherwise specified, all reagents were obtained from Sigma.

Clones and Mutants—The cloning of human *SKCa3* containing 19 polyglutamines in the N terminus (GenBank™ AF031815, AJ251016) and *IKCa1* (GenBank™ AF033021) has been reported previously (30–32). The full coding region of *SKCa1* was amplified from human brain total RNA using reverse transcriptase polymerase chain reaction (PCR) with an engineered 5′ *Hin*dIII site near the start codon and a 3′ *Bam*HI site near the termination codon and was cloned in-frame into the *pEGFP-C3* vector (CLONTECH, Palo Alto, CA) to create *GFP-SKCa1*. PCR was used to generate mutant SKCa3 channels (28). PCR products were digested with *Kpn*I and *Bam*HI and cloned into *Kpn*I and *Bam*HI-cut *GFP-SKCa3*. All clones were verified by sequencing. DNA for transfection was prepared with the QIAGEN (Valencia, CA) Miniprep kit. Human *SKCa2* in pcDNA3 was a generous gift from Dr. Bernard Attali (Tel Aviv University, Sackler School of Medicine, Israel).

Transfection of Constructs into Mammalian Cells—COS-7 cells were plated in culture chambers (5 × 10^5 cells/chamber), and 12–24 h later, cells were transiently transfected using FuGene™ 6 (Roche Molecular Biochemicals) with the respective DNA in serum-free OptiMEM medium (Life Technologies, Inc.) as per the manufacturer's recommended protocol. GFP-positive cells were used for electrophysiological studies at 48 h following transfection. Typical transfection efficiencies using this protocol were 40–70%. PC12 cells were plated overnight on glass coverslips prior to use. Cell lines stably expressing mKv1.1, mKv1.3, and hKv1.5, hSlo, and RBL cells expressing endogenous rKir 2.1 were used for the selectivity screen as described previously (28).

Electrophysiology—Cells were studied in the whole cell configuration of the patch clamp technique. The holding potential in all experiments was −80 mV. For measurement of IK_{Ca}, SK_{Ca}, and BK_{Ca} currents, we used an internal pipette solution containing (in mM) 145 potassium aspartate, 2 $MgCl_2$, 10 HEPES, 10 K_2EGTA, and 8.5 $CaCl_2$ (1 μM free Ca^{2+}), pH 7.2, 290–310 mOsm. K_V currents were recorded with a fluoride-based internal solution. To reduce currents from native chloride channels in COS-7, sodium aspartate Ringer was used as an external solution (in mM) 160 sodium aspartate, 4.5 KCl, 2 $CaCl_2$, 1 $MgCl_2$, and 5 HEPES, pH 7.4, 290–310 mOsm. For Jurkat T cells, potassium aspartate Ringer was used as an external solution with K^+ instead of Na^+ (164.5 mM K^+). SK_{Ca} currents were elicited by 200-ms voltage ramps from −120 to 40 mV applied every 10 s, and the reduction of slope conductance at −80 mV by the toxin was taken as a measure of channel block. BK_{Ca} currents were elicited by 200-ms voltage ramps from −80 to 80 mV applied every 30 s, and channel block measured at 35 mV. The inward rectifier (rKir 2.1) in RBL cells was studied in sodium aspartate Ringer with a potassium aspartate-based pipette solution containing 50 nM free Ca^{2+}.

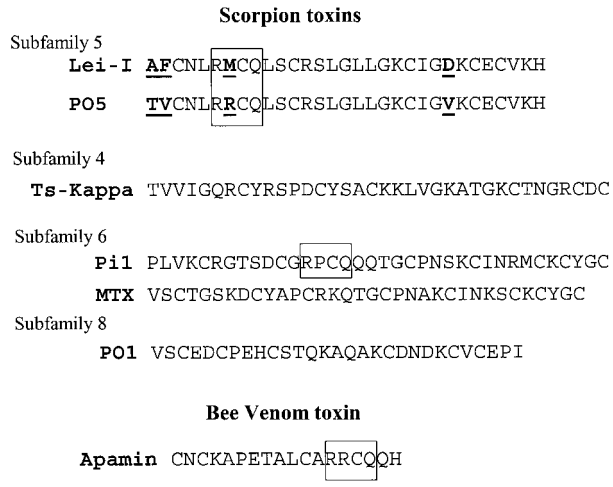

FIG. 1. **Sequence alignment of known** SK_{Ca} blockers showing subfamilies 4, 5, 6, and 8 from scorpion venom (28) and apamin. The conserved R*X*CQ motif is *boxed*. The differing residues of Lei and PO5 are *highlighted*. *MTX*, maurotoxin.

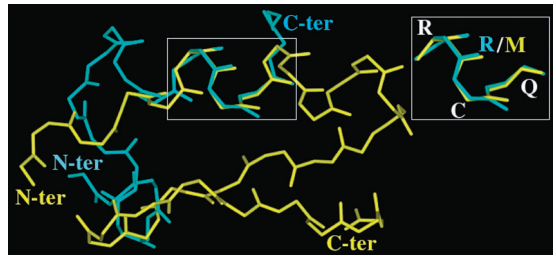

FIG. 2. **Superimposition of the backbone structures of Lei (*yellow*) and apamin (*blue*).** The R*X*CQ motif is *boxed*. *Inset*, R*X*CQ motif in both toxins on a larger scale.

Selective in Vivo Blockade of SKCa2 Channels by Lei-Dab^7 in Mice—Lei-Dab^7 was administered to 25-g C57/BL6 mice via the intracerebroventricular route, and the LD_{50} was determined (33). Groups of four mice per dose were injected with 5 μl of the peptide solution containing 0.1% (w/v) bovine serum albumin and 0.9% (w/v) sodium chloride.

RESULTS

Lei and PO5 Are Potent Inhibitors of Human SK_{Ca} Channels—Six peptide toxins from scorpion venom have been identified as SK_{Ca} channel blockers based on ^{125}I-apamin displacement studies on rat brain synaptosomes (34). Fig. 1 shows the sequence alignment of these toxins (35), three of which (Lei, PO5, and Pi1) contain a motif (R*X*CQ) reported to be important for binding to SK_{Ca} channels. (20, 36). Apamin contains an RRCQ sequence (Fig. 1), which has a spatial arrangement similar to that of the RMCQ motif in Lei (Fig. 2).

Lei is reported to block the well characterized human SKCa2 channel in Jurkat T cells with picomolar potency (15, 22, 23). As the first step in our strategy to design a specific SKCa2 inhibitor, we compared the potency of Lei with that of PO5, a toxin that differs from Lei only at positions 1, 2, 7, and 24 (Fig. 1), in blocking Jurkat SKCa2. Symmetric internal and external K^+ solutions were used to induce the inward component of the SKCa2 current. Following break-in with 1 μM Ca^{2+} in the pipette solution, SKCa2 currents were seen at negative potentials. At potentials more positive than −40 mV, K^+ currents were mainly due to Kv1.3 with minimal contribution from SKCa2 (Fig. 3*A*, *left*). The SKCa2 component was blocked by Lei and PO5, whereas the Kv1.3 current was unaffected (Fig. 3*A*, *left*). Dose-response curves showed that Lei blocked Jurkat SKCa2 with K_d values consistent with published data on the cloned and native channel (15, 22, 23) and with ~100-fold greater potency than PO5 (Fig. 3*B* and Table I). Lei and PO5

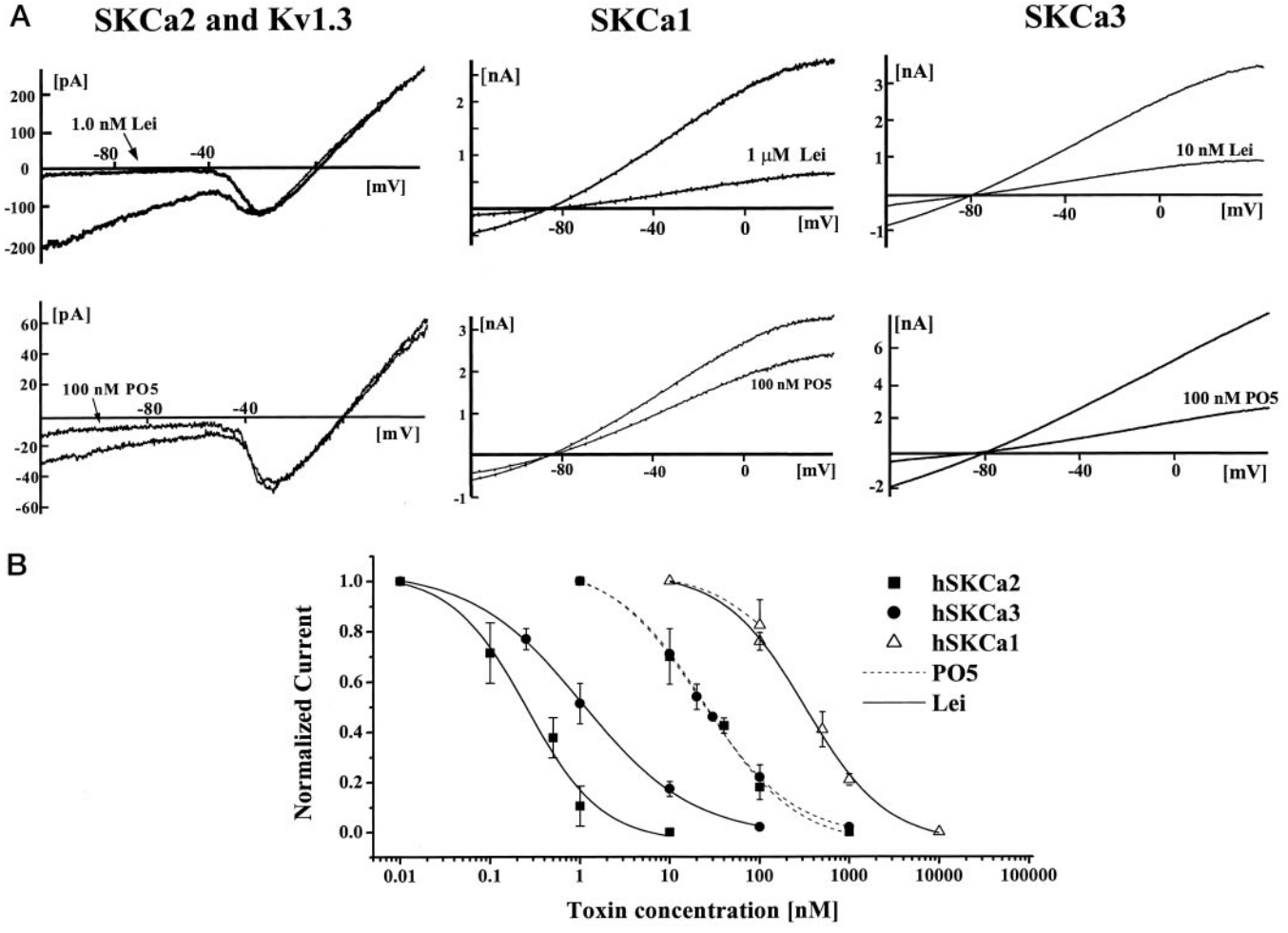

FIG. 3. **Effect of Lei and PO5 on SKCa1–3.** *A*, typical current traces on the three SK^+_{Ca} channels showing block with Lei and PO5. SKCa2 and Kv1.3 (*left*); SKCa1 (*middle*); SKCa3 (*right*). *B*, dose-response curves of Lei and PO5 on SKCa1–3. Lei on hSKCa1 (△, *straight line*, K_d = 325 nM); Lei on hSKCa2 (■, *straight line*, K_d = 0.2 nM); Lei on hSKCa3 (●, *straight line*, K_d = 1.1 nM); PO5 on hSKCa2 (■, *dashed line*, K_d = 22.1 nM); and PO5 on hSKCa3 (●, *dashed line*, K_d = 25.1 nM). Only one concentration of PO5 was tested on SKCa1 (shown). Typical SKCa1–3 currents were studied in the whole cell configuration of the patch clamp technique. Recordings were done with 1 μM free calcium as the internal pipette solution, and currents were elicited by voltage ramps from −120 to 40 mV. SKCa1 and SKCa3 were expressed transiently in COS-7 cells. An external solution containing sodium aspartate (5 mM potassium aspartate) was used for the recordings, and the degree of block was measured as the decrease in slope conductance at −80 mV. Jurkat T-cells were used to assess the effect on endogenous hSKCa2 with symmetric internal and external potassium aspartate (165 mM potassium aspartate).

TABLE I
Comparison of competition data on rat brain synaptosomes of indicated toxins (20, 34, 36) with K_d values by patch clamp on hSKCa2 and hSKCa3

Toxin	Source	^{125}I-displacement	*SKCa2* (Jurkat)	*SKCa3* (COS-7)
Leiurotoxin I (scyllatoxin)	*Leiurus quinquestriatus hebraeus*	N/A	0.2 ± 0.05 nM	1.1 ± 0.2 nM
PO5	*Androctonus mauretanicus mauretanicus*	20 pM	22 ± 0.5 nM	25 ± 2.5 nM
Tsκ	*Tityus serrulatus*	300 pM	80 ± 11 nM	197 ± 8 nM
Pi1-OH	*Pandinus imperator*	N/A	>1 μM	330 nM
Pi1-NH_2	*Pandinus imperator*	0.55 pM	100 ± 30 nM	250 nM
Maurotoxin (MTX)	*Scorpio maurus palmatus*	5–12 nM	1 μM	>1 μM
PO1	*Androctonus mauretanicus mauretanicus*	100 nM	>1 μM	>1 μM

were next evaluated on cloned SKCa1 and SKCa3 expressed in COS-7 cells. SKCa1 (Fig. 3*A*, *middle*) and SKCa3 (Fig. 3*A*, *right*) K^+ currents elicited with 1 μM Ca^{2+} in the pipette solution reversed at −80 mV in the presence of external sodium Ringer. Lei and PO5 blocked SKCa3 but were ineffective on SKCa1 (Fig. 3*A* and Table I). Comparison of the dose-response curves of SKCa3 showed Lei to be 25-fold more effective than PO5 (Fig. 3*B* and Table I). For reasons that remain unclear, four other scorpion toxins (maurotoxin, Pi1, PO1, and Tsκ) reported to be highly active in ^{125}I-apamin displacement assays (20, 34, 36) had little or no blocking activity on SKCa2 or SKCa3 (Table I). Thus, the two most potent scorpion peptides, Lei and PO5, exhibited significantly different blocking potencies on SKCa2 and SKCa3 despite differing at only four positions.

Ala^1*, Phe*^{2}*, and Met*^{7} *in Lei Are Responsible for the Enhanced Potency of Lei over PO5*—To define the residues responsible for the increased affinity of Lei for SK_{Ca} channels, we replaced each of the four differing residues in PO5 with the corresponding residue in Lei. PO5-V24D blocked SKCa2 and SKCa3 with a potency comparable with native PO5 (Fig. 4*A*). PO5-T1A, PO5-V2F, and PO5-R7M blocked SKCa2 with potencies approaching that of Lei. The improved potency of all three PO5 mutants to nearly that of Lei suggests that any of the indicated

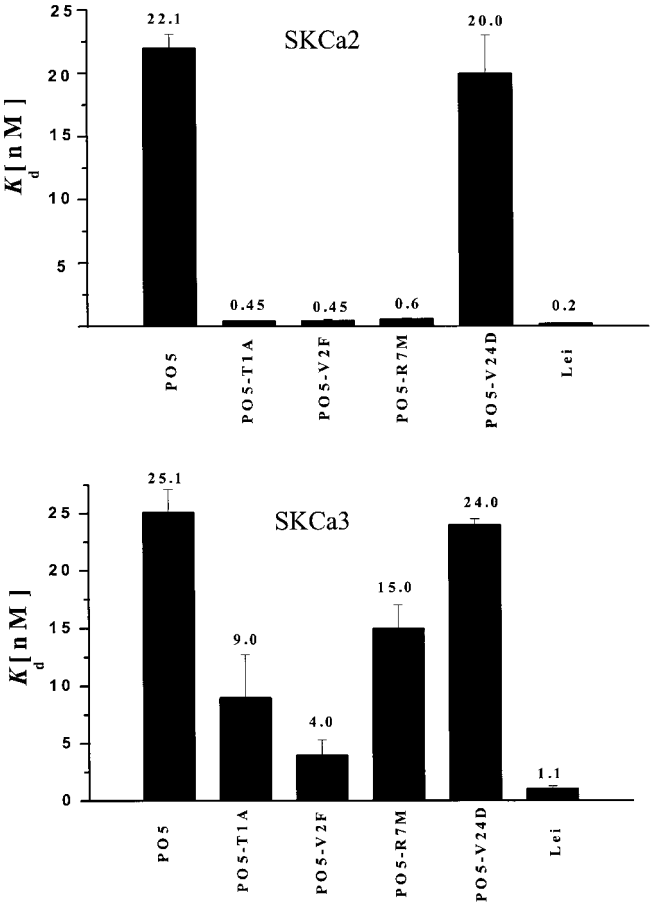

FIG. 4. **Histograms showing the effect of replacement of Thr^1, Val^2, Arg^7, and Val^{24} in PO5 with the corresponding residues in Lei in blocking SKCa2 (*A*) and SKCa3 (*B*).** The K_d values of native toxin is shown for comparison.

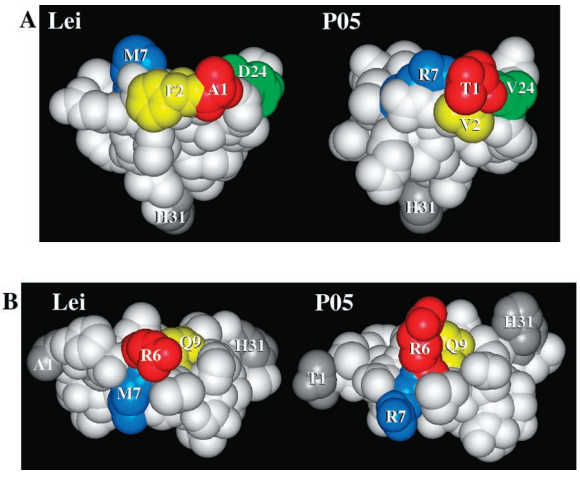

FIG. 5. **Space-filling models of Lei (*left*) and PO5 (*right*) showing residues at positions 1, 2, 7, and 24 (*A*) and the conserved R*X*CQ motif (*B*).** *X* = methionine in Lei and arginine in PO5.

Side chain at position 6	SKCa2	SKCa3
Native toxin-Arginine	0.2 ± 0.05 nM (n = 12)	1.1 ± 0.2 nM (n = 11)
Leucine	15 ± 0.3 nM (n = 5)	180 ± 38 nM (n = 5)
Citrulline	>> 1 μM (n = 4)	>> 1 μM (n = 4)
Lysine	4.5 ± 0.5 nM (n = 5)	36 ± 9.2 nM (n = 5)
Homo-Arginine	540 ± 40 nM (n = 5)	>1 μM (n = 3)

FIG. 6. **Effect of substitutions at position 6 of Lei in blocking SKCa2 (*left*) and SKCa3 (*right*).** The respective K_d values is shown on the *right*. *Numbers* in *parentheses* indicate the number of times tested.

alterations in the side chains at these positions may allow PO5 to fit more tightly within the channel-binding pocket due to either shorter side-chain size or local change in backbone conformation (37, 38). Similar results were obtained with these PO5 mutants on SKCa3 (Fig. 4*B*). The reverse mutation in Lei (Lei-M7R) reduced potency on both SKCa2 and SKCa3 (data not shown). These results indicate that Ala^1, Phe^2, and Met^7 underlie the increased affinity of Lei over PO5 for SKCa2 and SKCa3. These three residues form a localized binding pocket that may represent an important contact point with SK_{Ca} channels (Fig. 5, *A* and *B*).

Lei-Dab^7 *Is a Highly Selective Inhibitor of SKCa2*—Positions 6 and 7 of Lei are part of the conserved R*X*CQ motif (Fig. 1). To define the role of the residues in this motif, a series of Lei mutants was made at positions 6 and 7 to probe the toxin-channel interaction. Charge-neutralization mutations at position 6 that retained size (Arg^6 → leucine or citrulline) reduced toxin potency 70–180-fold for both channels (Fig. 6), indicating the need for a charged residue at this position. Substitution of the unbranched lysine at position 6, a mutation that retained charge but decreased size, also reduced toxin affinity for both channels (20–35-fold), whereas the introduction of the positively charged, bulky branched unnatural amino acid, homoarginine, caused a 1000-fold decrease in toxin potency (Fig. 6). Thus, substitutions at position 6 are not tolerated, and the arginine has the optimum size, charge, and branching required for interaction with SK_{Ca} channels. Furthermore, when residues at positions 6 and 7 were exchanged, the Lei-R6M+M7R double mutant was considerably less potent than the native toxin on SKCa2 and SKCa3 (K_d = 9.5 and 65 nM, respectively), establishing the importance of the relative locations of Arg^6 and Met^7 in the R*X*CQ motif.

We next turned our attention to position 7 in the R*X*CQ motif and found our first promising lead. Introduction of positively charged lysine at position 7 (Lei-M7K) yielded a mutant that blocked SKCa2 35-fold more potently than SKCa3 (Fig. 7). In an attempt to further enhance this difference, we generated two additional Lei mutants in which Met^7 was replaced by smaller positively charged unnatural amino acids diaminopropionate (Lei-Dapa^7) and diaminobutanoate (Lei-Dab^7). Lei-Dapa^7 blocked Jurkat SKCa2 ~350-fold more potently than SKCa3, whereas Lei-Dab^7 was ~650-fold more effective. Similar results

were obtained with the cloned SKCa2 channel expressed in COS-7 cells (Table II). Lei-Dab^7 was also ineffective against hSKCa1, hIKCa1, hSlo, K_V, and Kir channels, establishing its specificity for SKCa2 (Table II).

Asn^{367} in the SKCa2 Pore Region Is Important for Lei-Dab^7 Selectivity—Because Lei-Dab^7 and apamin share the critical R*X*CQ channel-binding motif (Figs. 1 and 2), it is likely that Lei-Dab^7, like apamin (39), binds to residues in the external S5-Pore-S6 region of the channel. Human SKCa2 and SKCa3 differ at only two positions in the pore region (Fig. 8*A*). To determine whether one or both these residues contribute to Lei-Dab^7 selectivity (Fig. 8, *B* and *C*), we replaced these two residues in SKCa3 (Val^{485} and His^{521}) with the corresponding residues of SKCa2 (Ala^{331} and Asn^{367}), individually or together. Lei-Dab^7 blocked SKCa3-H521N (K_d = 20 ± 4.7 nM) and SKCa3-V485A + H521N (K_d = 7.5 ± 1.2 nM) with nearly the same potency as SKCa2 (Fig. 8, *D* and *E*, and Table II), whereas SKCa3-V485A did not produce functional channels. In mutant cycle studies with the SKCa3-H521N and SKCa3-V485A+H521N mutants, residue 7 of Lei-Dab^7 was found to couple tightly with His^{521} ($\Delta\Delta G$ = 2.4), suggesting that these two residues lie in close proximity to each other. We conclude that Lei-Dab^7 binds to the external vestibule of SK_{Ca} channels and that Asn^{367} (the residue corresponding to His^{521} of hSKCa3) in SKCa2 contributes to Lei-Dab^7 selectivity.

Selective in Vivo Blockade of Homotetrameric SKCa2 Channels by Lei-Dab^7 Does Not Cause Gross Neurotoxicity—To evaluate the central nervous system effects of specific *in vivo* blockade of SKCa2 homotetramers, Lei-Dab^7 was administered via the intracerebroventricular route to mice. At a concentration (10 ng (or 300 nM assuming a brain liquid volume of 10 μl)) that would selectively block >99% of SKCa2 homotetramers, no gross central nervous system toxicity was

Side chain at position 7	SKCa2	SKCa3
Native toxin -Methionine	0.2 ± 0.05 nM (n = 12)	1.1 ± 0.2 nM (n = 11)
Leucine	0.55 ± 0.05 nM (n = 5)	6 ± 4.7 nM (n = 5)
Lysine	3 ± 0.5 nM (n = 5)	105 ± 20 nM (n = 6)
Dapa	5.5 ± 0.8 nM (n = 5)	2000 ± 300 nM (n = 4)
Dab	3.8 ± 1.1 nM (n = 11)	2500 ± 500 nM (n = 5)

FIG. 7. **Effect of substitutions at position 7 of Lei in blocking SKCa2 (*left*) and SKCa3 (*right*).** The respective K_d values is shown on the *right*. *Numbers* in *parentheses* indicate the number of times tested.

TABLE II
Selectivity of Lei-Dab7 on a panel of channels K_d indicated on the right

Channel	Lei-Dab^7 K_d
K_{Ca} channels	
hSKCa1	6000 ± 800 nM
hSKCa2 (Jurkat)	3.8 ± 0.5 nM
hSKCa2 (cloned)	5.5 ± 0.7 nM
hSKCa3	2500 ± 500 nM
hIKCa1	No effect at 1 μM
hSlo	No effect at 1 μM
K_V channels	
mKv1.1	No effect at 1 μM
mKv1.3 (cloned)	No effect at 1 μM
hKv1.3 (Jurkat)	No effect at 1 μM
hKv1.5	No effect at 1 μM
rKv1.2 and Kv2.1 (PC12)	No effect at 1 μM
Inward rectifier	
rKir2.1 (RBL cells)	No effect at 1 μM

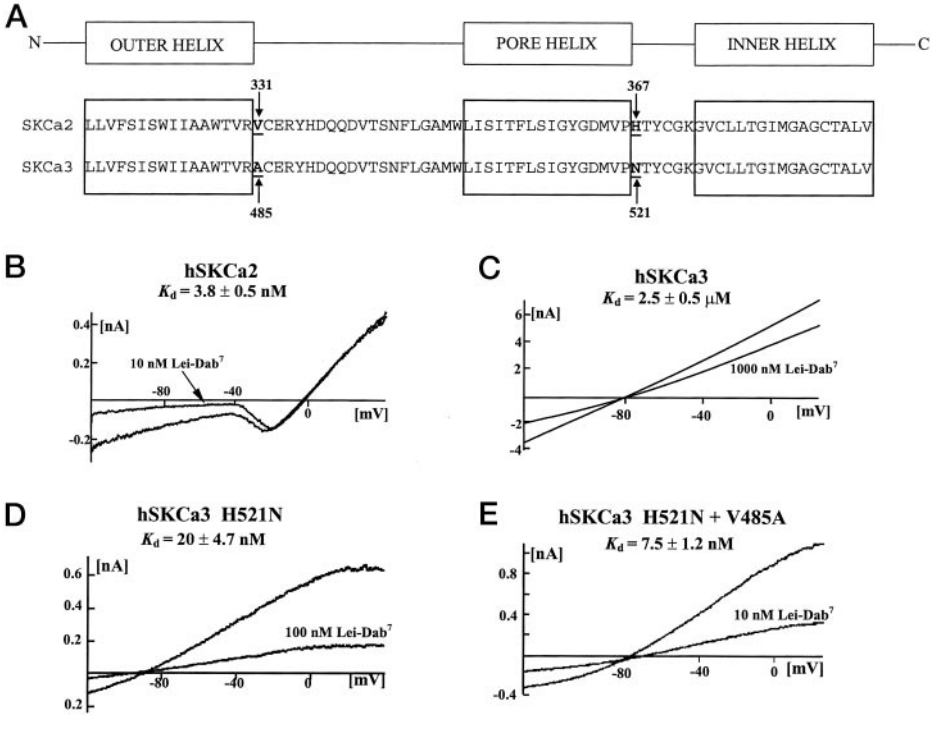

FIG. 8. **Effect of replacement of differing residues in the S5-Pore-S6 region in SKCa3 with the corresponding residues in SKCa2.** *A*, sequence alignment of SKCa2 and SKCa3 S5-Pore-S6 region with the two differing residues *underlined*. *B*, 10 nM Lei-Dab^7 on native SKCa2 (K_d = 3.8 nM ± 0.5 nM). *C*, 1000 nM Lei-Dab^7 on hSKCa3 (K_d = 2500 ± 500 nM). *D*, 100 nM Lei-Dab^7 on hSKCa3-H521N (K_d = 20 ± 4.7 nM). *E*, 10 nM Lei-Dab^7 on hSKCa3-V485A+H521N (K_d = 7.5 nM ± 1.2 nM).

observed. At a higher concentration (50 ng (or 1500 nM)), all six animals became hyperexcitable, developed convulsions followed by paralysis lasting 15 h, and then fully recovered. At much higher concentrations (80 ng (or 2400 nM)), 50% of the animals died within 2 h, and 100% lethality was observed in 1 h at 100 ng (3 μM). The neurotoxicity observed at Lei-Dab^7 concentrations higher than 1500 nM may be due to the blockade of SKCa1 and/or SKCa3 homotetrameric channels (Table II), although we cannot exclude the contribution of heteromultimeric SK_{Ca} channels containing SKCa2 subunits.

DISCUSSION

Functional SK_{Ca} channels are tetramers of SKCa1–3 subunits that can assemble as homo- or heterooligomers (39). Heterooligomers are likely to exist natively given the overlapping patterns of distribution of SKCa1–3 in the central nervous system. SKCa1 and SKCa2 are abundant in the hippocampus, whereas the medial habenula has both SKCa2 and SKCa3 (10, 16). The available SK_{Ca} channel inhibitors, including apamin (3, 22, 25, 26) and the UCL compounds (7, 25), do not have the requisite selectivity to define the specific functional roles of the homo- and heterooligomeric SK_{Ca} channels present in mammalian tissues. In this study, we used a structure-guided approach to develop Lei-Dab^7, a novel peptide that blocks SKCa2 homotetramers with nanomolar potency and exhibits 650-fold or greater selectivity over related homooligomeric channels. Heterooligomeric SK_{Ca} channels may exhibit intermediate sensitivity for Lei-Dab^7 compared with their homotetrameric counterparts as has been shown with apamin on recombinant heterotetramers of SKCa1 and SKCa2 (39).

Lei-Dab^7 might help elucidate the contributions of SKCa2 channels in mediating neuronal afterhyperpolarization (3–5) and in the apamin-induced destruction of cerebellar Purkinje neurons (17) and altered seizure threshold (18, 19). Lei-Dab^7 may also help define the role of SKCa2 in the retina, liver, melanocytes, immune system, and fetal heart. The subunit composition of SK_{Ca} heterooligomers in diverse mammalian tissues may also be determined by using Lei-Dab^7 in much the same way as radiolabeled peptide toxins selective for a particular K_V subunit have proven useful in assessing the subunit composition of brain heteromeric K_V channels (40–42).

Peptide inhibitors of SK_{Ca} channels form a structurally distinct group and lack the conserved dyad present in peptide blockers of K_V, IKCa1, and BK_{Ca} channels that consists of an aromatic residue with a neighboring invariant lysine (43). Therefore, the architecture of the toxin-binding surface in the external vestibule of SK_{Ca} channels may differ from that of K_V (44–47) and IKCa1 (28, 48) channels, which are similar to that of the crystallographically defined structure of the bacterial K^+ channel, KcsA (49, 50). The topologies of K_V and IKCa1 channels were deduced from toxin mapping studies by identifying multiple contact points between toxins of known structure and these channels. Lei-Dab^7 may similarly be used as a molecular caliper to delineate the architecture of the external vestibule of SKCa2 . Molecular models of SK_{Ca} channels based on complementary mutagenesis studies would facilitate the development of selective and potent inhibitors of SKCa1 and SKCa3.

Acknowledgments—We thank Chialing Wu and Dr. Luette Forrest for technical assistance, Dr. Pascal Mansuelle for amino acid analyses and Edman sequencing, and Prof. Herve Rochat for constant support.

REFERENCES

1. Latorre, R., Oberhauser, A., Labarca, P., and Alvarez, O. (1989) *Annu. Rev. Physiol.* **51,** 385–399
2. Hirschberg, B., Maylie, J., Adelman, J. P., and Marrion, N. V. (1998) *J. Gen. Physiol.* **111,** 565–581
3. Kohler, M., Hirschberg, B., Bond, C. T., Kinzie, J. M., Marrion, N. V., Maylie, J., and Adelman, J. P. (1996) *Science* **273,** 1709–1714
4. Sah, P. (1996) *Trends Neurosci.* **19,** 150–154
5. Xia, X. M., Fakler, B., Rivard, A., Wayman, G., Johnson-Pais, T., Keen, J. E., Ishii, T., Hirschberg, B., Bond, C. T., Lutsenko, S., Maylie, J., and Adelman, J. P. (1998) *Nature* **395,** 503–507
6. Barfod, E. T., Moore, A. L., and Lidofsky, S. D. (2001) *Am. J. Physiol.* **280,** C836–C842
7. Fanger, C. M., Rauer, H., Neben, A. L., Miller, M. J., Rauer, H., Wulff, H., Rosa, J. C., Ganellin, C. R., Chandy, K. G., and Cahalan, M. D. (2001) *J. Biol. Chem.* **276,** 12249–12256
8. Pribnow, D., Johnson-Pais, T., Bond, C. T., Keen, J., Johnson, R. A., Janowsky, A., Silvia, C., Thayer, M., Maylie, J., and Adelman, J. P. (1999) *Muscle Nerve* **22,** 742–750
9. Kimura, T., Takahashi, M. P., Okuda, Y., Kaido, M., Fujimura, H., Yanagihara, T., and Sakoda, S. (2000) *Neurosci. Lett.* **295,** 93–96
10. Rimini, R., Rimland, J. M., and Terstappen, G. C. (2000) *Brain Res.* **85,** 218–220
11. Jenkinson, D. H., Haylett, D. G., and Cook, N. S. (1983) *Cell Calcium* **4,** 429–437
12. Paolocci, N., Pagliaro, P., Isoda, T., Saavedra, F. W., and Kass, D. A. (2001) *Circulation* **103,** 119–124
13. Nagayama, T., Fukushima, Y., Hikichi, H., Yoshida, M., Suzuki-Kusaba, M., Hisa, H., Kimura, T., and Satoh, S. (2000) *Am. J. Physiol.* **279,** R1731–R1736
14. Grissmer, S., Lewis, R. S., and Cahalan, M. D. (1992) *J. Gen. Physiol.* **99,** 63–84
15. Hanselmann, C., and Grissmer, S. (1996) *J. Physiol. (Lond.)* **496,** 627–637
16. Stocker, M., and Pedarzani, P. (2000) *Mol. Cell. Neurosci.* **15,** 476–493
17. Mourre, C., Fournier, C., and Soumireu-Mourat, B. (1997) *Brain Res.* **778,** 405–408
18. McCown, T. J., and Breese, G. R. (1990) *Eur. J. Pharmacol.* **187,** 49–58
19. Empson, R., and Jefferys, J. (2001) *Neuroscience* **102,** 297–306
20. Sabatier, J. M., Fremont, V., Mabrouk, K., Crest, M., Darbon, H., Rochat, H., Van Rietschoten, J., and Martin-Eauclaire, M. F. (1994) *Int. J. Pept. Protein Res.* **43,** 486–495
21. Klocker, N., Oliver, D., Ruppersberg, J., Knaus, H., and Fakler, B. (2001) *Mol. Cell. Neurosci.* **17,** 514–520
22. Desai, R., Peretz, A., Idelson, H., Lazarovici, P., and Attali, B. (2000) *J. Biol. Chem.* **275,** 39954–39963
23. Jaeger, H., Adelman, J. P., and Grissmer, S. (2000) *FEBS Lett.* **469,** 196–202
24. Grissmer, S., Nguyen, A. N., and Cahalan, M. D. (1993) *J. Gen. Physiol.* **102,** 601–630
25. Stroebaek, D., Joergensen, T. D., Christophersen, P., Ahring, P. K., and Olesen, S. P. (2000) *Br. J. Pharmacol.* **129,** 991–999
26. Shah, M., and Haylett, D. G. (2000) *Br. J. Pharmacol.* **129,** 627–630
27. Kalman, K., Pennington, M. W., Lanigan, M. D., Nguyen, A., Rauer, H., Mahnir, V., Paschetto, K., Kem, W. R., Grissmer, S., Gutman, G. A., Christian, E. P., Cahalan, M. D., Norton, R. S., and Chandy, K. G. (1998) *J. Biol. Chem.* **273,** 32697–32707
28. Rauer, H., Lanigan, M. D., Pennington, M. W., Aiyar, J., Ghanshani, S., Cahalan, M. D., Norton, R. S., and Chandy, K. G. (2000) *J. Biol. Chem.* **275,** 1201–1208
29. Merrifield, B. (1986) *Science* **232,** 341–347
30. Chandy, K. G., Fantino, E., Wittekindt, O., Kalman, K., Tong, L. L., Ho, T. H., Gutman, G. A., Crocq, M. A., Ganguli, R., Nimgaonkar, V., Morris-Rosendahl, D. J., and Gargus, J. J. (1998) *Mol. Psychiatry* **3,** 32–37
31. Logsdon, N. J., Kang, J., Togo, J. A., Christian, E. P., and Aiyar, J. (1997) *J. Biol. Chem.* **272,** 32723–32726
32. Ghanshani, S., Coleman, M., Gustavsson, P., Wu, A. C., Gargus, J. J., Gutman, G. A., Dahl, N., Mohrenweiser, H., and Chandy, K. G. (1998) *Genomics* **51,** 160–161
33. Behrens, B., and Karber, C. (1935) *Arch. Exp. Pathol. Pharmakol.* **177,** 379–388
34. Fajloun, Z., Carlier, E., Lecomte, C., Geib, S., Di Luccio, E., Bichet, D., Mabrouk, K., Rochat, H., De Waard, M., and Sabatier, J. M. (2000) *Eur. J. Biochem.* **267,** 5149–5155
35. Tytgat, J., Chandy, K., Garcia, M., Gutman, G., Martin-Eauclaire, M., van der Walt, J., and Possani, L. (2000) *Trends Pharmacol. Sci.* **20,** 444–447
36. Sabatier, J. M., Zerrouk, H., Darbon, H., Mabrouk, K., Benslimane, A., Rochat, H., Martin-Eauclaire, M. F., and Van Rietschoten, J. (1993) *Biochemistry* **32,** 2763–2770
37. Rajamohan, F., Alzate, O., Cotrill, J. A., Curtiss, A., and Dean, D. H. (1996) *Proc. Natl. Acad. Sci. U. S. A.* **93,** 14338–14343
38. Smith, L. A., Reid, P. F., Wang, F. C., Parcej, D. N., Schmidt, J. J., Olson, M. A., and Dolly, J. O. (1997) *Biochemistry* **36,** 7690–7696
39. Ishii, T. M., Maylie, J., and Adelman, J. P. (1997) *J. Biol. Chem.* **272,** 23195–23200
40. Scott, V. E., Muniz, Z. M., Sewing, S., Lichtinghagen, R., Parcej, D. N., Pongs, O., and Dolly, J. O. (1994) *Biochemistry* **33,** 1617–1623
41. Koschak, A., Bugianesi, R. M., Mitterdorfer, J., Kaczorowski, G. J., Garcia, M. L., and Knaus, H. G. (1998) *J. Biol. Chem.* **273,** 2639–2644
42. Koch, R. O., Wanner, S. G., Koschak, A., Hanner, M., Schwarzer, C., Kaczorowski, G. J., Slaughter, R. S., Garcia, M. L., and Knaus, H. G. (1997) *J. Biol. Chem.* **272,** 27577–27581
43. Dauplais, M., Lecoq, A., Song, J., Cotton, J., Jamin, N., Gilquin, B., Roumestand, C., Vita, C., de Medeiros, C. L. C., Rowan, E. G., Harvey, A. L.,

and Menez, A. (1997) *J. Biol. Chem.* **272,** 4302–4309
44. Aiyar, J., Withka, J. M., Rizzi, J. P., Singleton, D. H., Andrews, G. C., Lin, W., Boyd, J., Hanson, D. C., Simon, M., Dethlefs, B., Lee, C.-L., Hall, J. E., Gutman, G. A., and Chandy, K. G. (1995) *Neuron* **15,** 1169–1181
45. Aiyar, J., Rizzi, J. P., Gutman, G. A., and Chandy, K. G. (1996) *J. Biol. Chem.* **271,** 31013–31016
46. Hidalgo, P., and MacKinnon, R. (1995) *Science* **268,** 307–310
47. Ranganathan, R., Lewis, J. H., and MacKinnon, R. (1996) *Neuron* **16,** 131–139
48. Rauer, H., Pennington, M., Cahalan, M., and Chandy, K. G. (1999) *J. Biol. Chem.* **274,** 21885–21892
49. Doyle, D. A., Morais Cabral, J., Pfuetzner, R. A., Kuo, A., Gulbis, J. M., Cohen, S. L., Chait, B. T., and MacKinnon, R. (1998) *Science* **280,** 69–77
50. MacKinnon, R., Cohen, S. L., Kuo, A., Lee, A., and Chait, B. T. (1998) *Science* **280,** 106–109